iomac
International Operational Modal Analysis Conference

11th International Operational Modal Analysis Conference

20 - 23 May 2025 | Rennes, France

Application of Gyroscopes for Stability Monitoring in Flutter Tests

Martin Tang [1], *Keith Soal* [2], *Marc Böswald* [3] *and Yves Govers* [4]

[1] German Aerospace Center, Institute of Aeroelasticity, Bunsenstraße 10, 37085 Gottingen, Germany, martin.tang@dlr.de
[2] German Aerospace Center, Institute of Aeroelasticity, Bunsenstraße 10, 37085 Gottingen, Germany, keith.soal@dlr.de
[3] German Aerospace Center, Institute of Aeroelasticity, Bunsenstraße 10, 37085 Gottingen, Germany, marc.boeswald@dlr.de
[4] German Aerospace Center, Institute of Aeroelasticity, Bunsenstraße 10, 37085 Gottingen, Germany, yves.govers@dlr.de

ABSTRACT

Accelerations are in most cases used to track modal parameters of vehicles in operation. In flutter flight tests, these modal parameters are used to ensure safety during flight. Recently, low cost MEMS sensors became popular for application in drones, where apart from acceleration also rotation rates are measured. This work investigates whether this quantity is also able to track the modal parameters. Data from the P-Flex model is utilized to study the rotation rate responses. First, data is analyzed from ground tests. In a second step, flight tests are analyzed. To improve results, virtual references are introduced to reduce complexity of the responses and modes are separated into symmetric and anti-symmetric. Results from ground tests show the applicability and also during flight, modes are tracked successfully. Nevertheless, due to significant noise and limited measurement time for noise reduction through averaging, there is room for improvement regarding the damping estimates.

Keywords: Flight Vibration Test, Flutter Monitoring, Gyroscopes, Modal Rotations

1. INTRODUCTION

A phenomena called flutter is an unstable state in flight, where aircraft experiences self-induced vibrations causing the structure to fail. Monitoring of airframes, e.g. through Operational Modal Analysis (OMA), is a common approach to ensure aeroelastic stability in flight [1]. Recently, MEMS sensors have become more and more popular enabling the measurement of rate of rotations [2]. This work investigates whether those rates of rotation enable the tracking of aeroelastic stability with OMA.

2. THEORETICAL BACKGROUND

In this section, modal rotations are introduced. An analytical model of a wing-like structure is used for this purpose, with the requirement to observe bending and torsion deformation. Following, modal identification procedures for OMA in frequency domain are outlined.

2.1. Modal Rotations

In finite element analysis, many different structural elements are available for simulations. For some elements, e.g. plates and beams, rotational degrees of freedom are required to express the internal displacements with regard to the discrete displacements at the element nodes. Hence, rotational degrees of freedom are already available for numerical modal analysis, as indicated in Figure 1.

A plate model of a wing-like structure is modeled and analyzed in order to plot rotational degrees of freedom and to compare the result with translational deflection. The model is a tapered and cantilevered flat plate, made of steel, with a thickness of $3.5\,\mathrm{mm}$, spanwidth of $794\,\mathrm{mm}$, chord width at the root of $310\,\mathrm{mm}$ and chord width at the tip of $100\,\mathrm{mm}$. The chord direction is discretized in 10 elements and the span direction is discretized in 40 elements. A simulation model in MSC.Nastran has been set up with CQUAD4 elements as depicted in Figure 2.

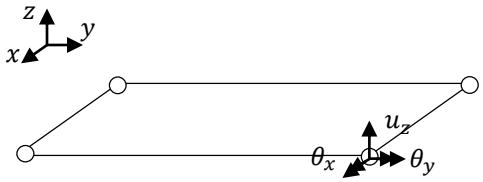

Figure 1: Degrees of freedom of a single plate element.

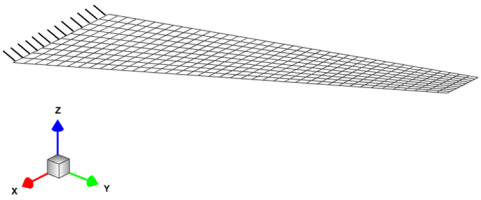

Figure 2: Finite element model of the cantilevered tapered plate.

The first four modes, consisting of three bending modes and one torsion mode, are presented in Figure 3 with rotational and translational deflection. All degrees of freedom are normalized to maximum displacement equals 1. Since all degrees of freedom result from the same modal vector in the eigenvalue analysis, the common normalization of all deflection types for each mode shape vector is mathematically consistent, although physical units do not cancel out. First bending is shown in Figure 3a and θ_x shows surprisingly the largest response. Figure 3c plots the torsion mode and it is seen that θ_y allows the observation of torsion at the center line, while the deflection u_z is not able to indicate torsion.

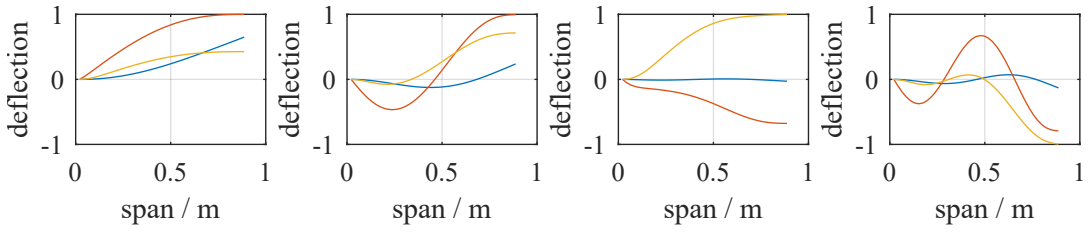

(a) first bending **(b)** second bending **(c)** torsion **(d)** third bending

Figure 3: Mode shapes for plate model at center line. Blue: u_z; Red: θ_x; Yellow: θ_y.

This example shows that the rotational degrees of freedom θ_x and θ_y alone are able to indicate bending and torsion along the elastic axis of the plate. Figure 4 presents the FRFs at the mid point of the plate for excitation at the tip. u_z is shown as accelerance, while the rotations θ_x and θ_y are shown as mobility. The four peaks correspond to the four modes shown in Figure 3. All bending modes are well represented in θ_x whereas the torsion mode around $55\,\mathrm{Hz}$ is best observed in θ_y. As a result, torsion is easier detected with θ_y and bending is easier detected with θ_y.

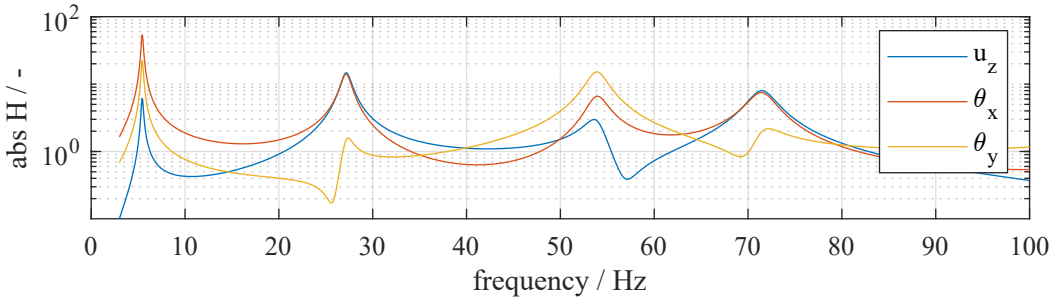

Figure 4: Frequency response function for all deflection types at the midpoint of the plate.

3. METHODOLOGY

The process for monitoring of modal parameters is outlined in this section. In addition, an approach is proposed to reduce analysis complexity for better modal identification.

3.1. Modal Tracking

In OMA modal properties of a structure are estimated during operation. With those properties, the state of the structure is monitored. Hence, a linear time invariant (LTI) system is assumed. For this work, a method in frequency domain is utilized. Cross Power Spectral Densities (CPSD) are estimated first and subsequently a Least Squares Complex Frequency Domain (LSCF) approach is used to identify the poles of the system followed by a Least Squares Frequency Domain (LSFD) algorithm to compute the mode shapes [3].

The CPSDs are computed with the Welch method, meaning an averaging is taking place to smooth the spectral estimate. In order to compute the CPSDs, one or multiple reference signals are chosen. After application of modal analysis theory, the CPSDs can be expressed as a summation of poles and residues [4]. With LSCF, the polynomials are identified and the poles in terms of eigenfrequency and damping are computed as roots of the denominator. In a second step, the mode shapes are then fitted with the known poles to the estimated CPSDs.

In the scope of an online monitoring of modal parameters, the analysis is repeated after a chosen time period and for each analysis the modes are tracked with the MACXP criterion. This allows to observe the evolution of a specific mode over time. When an external parameter like flight speed is measured as well, then the mode and damping ratio is plotted against flight speed, allowing predictions for the next flight speed whether the aircraft remains stable or not.

3.2. Reduction of Modal Density

The use of accelerometers for in-flight identification of modal parameters is state of the art, as for example presented by Volkmar et al. [1]. This work investigates, whether the use of gyroscopes as an alternative sensor technology is also appropriate to identify and monitor the modal parameters of an aircraft.

Due to noisy response data and high modal density of airframes, two closely spaced poles are easily smeared into one resulting in additional challenges to the identification process. Furthermore, it will be investigated, if the use of gyroscopes can help to reduce the modal density for OMA. As can be seen in Figure 4, some modes are observed better in one rotational degree of freedom, while some other modes are better observed in another rotational degree of freedom. Furthermore, aircraft structure show symmetric and anti-symmetric modes which are separated if two or more signals are combined correctly into virtual responses [5]. If the different signals are separately used as reference for computation of CPSDs, reduced model orders are applied in each modal analysis helping improve the data quality.

4. APPLICATION

The FLIPASED EU-project has been set up to demonstrate applicability of control strategies to actively suppress flutter [6, 7]. The fixed-wing UAV P-Flex has been designed and manufactured for this purpose and tested in a GVT and FVT within the research program. Firstly, the results for the modal analysis with the gyroscopes responses are shown for the GVT with known inputs but nonetheless analyzed with methods from OMA. Secondly, the methodology is applied to the flutter flight tests.

4.1. GVT

The Flipased GVT is shown in Figure 5. The UAV is softly suspended in bungees to reproduce free flying conditions and excitation is introduced with electromagnetic shakers. External glued piezoelectric transducers to measure the response acceleration. For the current study, internal MEMS sensors with integrated gyroscopes are used to investigate the suitability of rate of rotation measurements for modal analysis to identify the modes of interest.

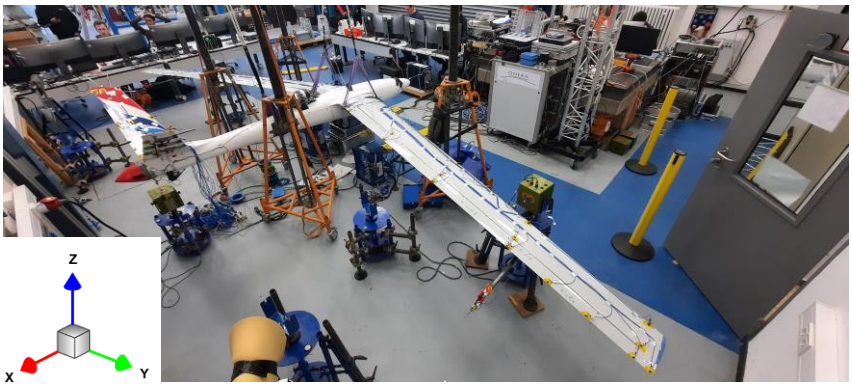

Figure 5: Setup for the Flipased GVT

From the flutter analysis it was found that the flutter mechanism is either a coupling between symmetric torsion with second symmetric bending or anti-symmetric torsion with first anti-symmetric bending. Random excitation at the wing in bending direction is thus analyzed.

In order to compute the virtual responses, the wing tip sensors are simply added to suppress anti-symmetric modes or subtracted in order to suppress symmetric modes. If θ_y is used as reference, the torsion modes should be emphasized and with θ_x as reference, the bending modes are emphasized. The resulting summed CPSDs are presented in Figure 6. In blue is the estimated APSD for all rotational sensors. This curve should clearly indicated the resonance peaks of all modes (i.e. high modal density). Red plots the result, where the reference is set up for symmetric bending modes. Yellow shows the anti-symmetric bending, purple should emphasize symmetric torsion modes and green the anti-symmetric torsion modes, respectively. The first peaks below 2 Hz represent the rigid body modes. The first one is the aircraft roll mode which is emphasized by the anti-symmetric references, while the other attenuate

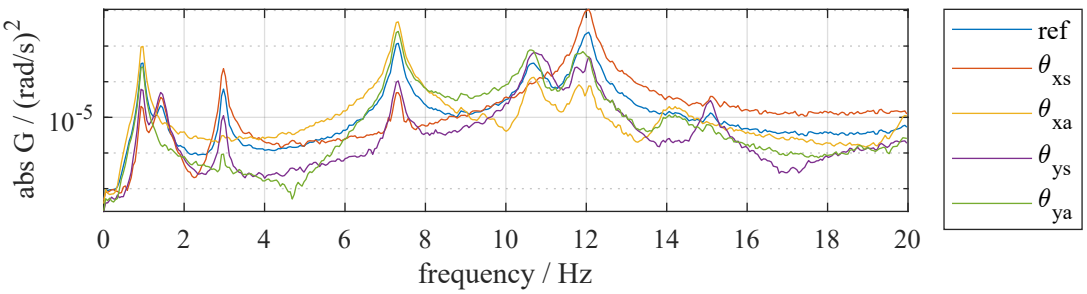

Figure 6: Sum CPSDs with different references.

this mode. The mode around 3 Hz represents the first symmetric wing bending which is emphasized by the red line, representing the reference for symmetric bending. In the yellow line, representing the reference for the anti-symmetric bending, this mode is not seen at all. Around 7 Hz the first anti-symmetric bending is seen and filtered by the purple and red curves representing the symmetric modes. Green and yellow are highlighting this mode, meaning that also a torsion participation is expected. Green and purple show a common peak around 11 Hz meaning that a torsion is expected there. The identified modes are summarized in Table 1.

Table 1: Modes from GVT.

Mode	Eigenfrequency / Hz	Damping / %
a/c roll	0.95	3.2
first symmetric bending	2.96	0.2
anti-symmetric bending	7.30	1.0
torsion right	10.66	0.6
torsion left	11.71	0.3
second symmetric bending	12.01	0.8

Mode shapes and respective sensor locations are shown in Figure 7. Instead of normal arrows, in this case two headed arrows are chosen, where the rotation is defined around the arrow with the right hand rule. Red arrows represent θ_x and therefore bending motion, while green arrows represent θ_y and hence torsion motion. Figure 7a depicts the first anti-symmetric bending. Attributed to the definition of rotation in arrows, the plot is symmetric. According to the mode shape, the right wing tip moves up, following the rotation, while the left wing tip moves down due to the same rotation direction. The mode shape also shows that an anti-symmetric torsion deformation is participating according to the green arrows. Figure 7b presents the second symmetric bending, while the θ_y arrows show an anti-symmetric structure. Figure 7c and 7d show the torsion modes. Unfortunately, it is seen that no symmetric or anti-symmetric behavior is measured but an asymmetric behavior. Both wings exhibit a torsion mode independent from each side, resulting that only one wing twists at a time.

This first investigation demonstrates that the approach to separate the symmetric and anti-symmetric mode shapes is applicable for the GVT measurements. The separation of bending and torsion however, is not fully applicable since both motions are also coupled.

4.2. FVT

Finally, the approach is applied to flight test data of the open loop flight test campaign to find the actual flutter speed of the vehicle [8]. During the flutter test flight, the altitude was kept constant at $365\,\mathrm{m}$ and the flight speed has been increased from $43\,\mathrm{m\,s^{-1}}$ to $54\,\mathrm{m\,s^{-1}}$ in 7 steps, and conditions were kept constant for roughly $2\,\mathrm{min}$.

For the post processing with the proposed method, the data is cut into segments with constant conditions and four virtual reference signals are computed in order to produce the required CPSDs. The procedure is depicted in Figure 8, where for each segment different CPSDs are computed with the virtual responses and all are merged into one modal data set for one flight speed. This is repeated for each segment corresponding to one flight speed, finally resulting in flight speed dependent modal parameters.

Figure 9 presents the result for the tracking of modal parameters during the flight test. All results of a given flight speeds have been merged and variances are computed for the different identifications of the same mode. If the variance is zero, only one mode has been found through all analysis and the variance is therefore not computed. It is seen that the purple line, which corresponds to a torsion mode drops in damping. However, the damping increases with the last flight speed but variance also increases. Through dominance of the flutter mode, it becomes also visible to the other virtual references, but identification becomes uncertain resulting in the high variance. It is also seen that the green line, corresponding to the other torsion also decreases in damping and is likely to become the second unstable mode. The bending modes are depicted by the red and yellow lines.

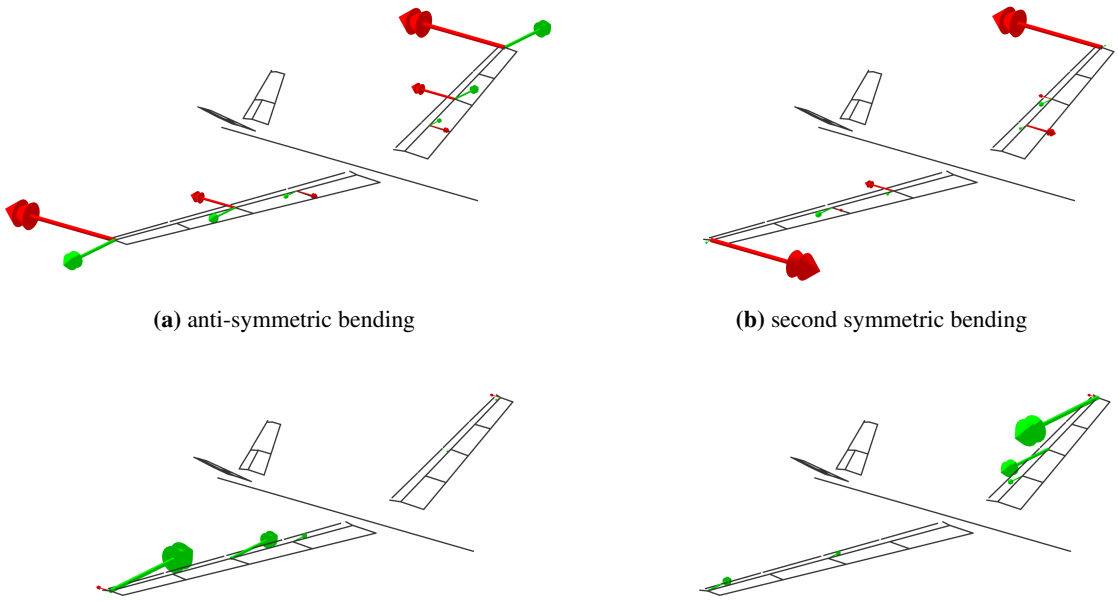

(a) anti-symmetric bending

(b) second symmetric bending

(c) torsion right

(d) torsion left

Figure 7: Rotational mode shapes for Flipased drone

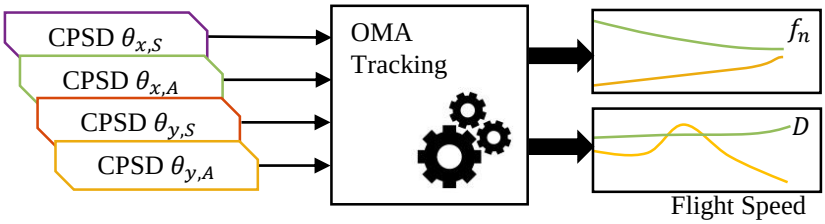

Figure 8: Schematic of identification procedure

5. CONCLUSIONS

It has been shown that modal rotations are able to detect torsion and bending of a wing, first in a theoretical model and then on the P-Flex testbed. Through the introduction of virtual reference signals, it is possible to separate symmetric and anti-symmetric modes. The rotation around the spanwise axis is able to detect torsion while the rotation around the chordwise axis is able to detect bending. Identification of different modes is practically conducted in separate modal analysis runs, each with reduced model order in the identification process. This simplifies modal identification and is then merged back into one modal model, which is plotted against flight speed.

One challenge however, is the noise due to short measurement times. The analysis could be further improved if a fusion algorithm merges the different mode sets including uncertainty for each identification [9]. Additionally, these modal rotations can be fused with the acceleration data. As for the modal identification, the virtual references can be utilized for time domain methods, like SSI as well, where better damping estimates are expected [8]. Nevertheless, it has been shown that the proposed methodology is able to successfully track modes in measured data.

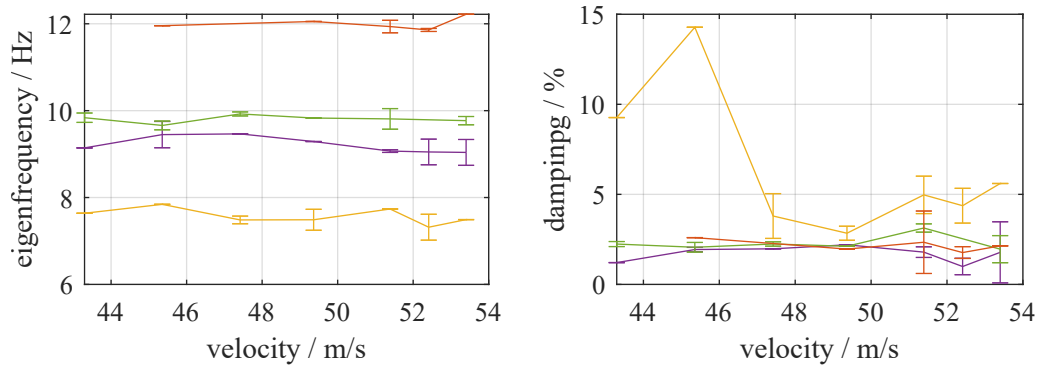

Figure 9: Stability diagram for flutter flight

REFERENCES

[1] Robin Volkmar et. al. Reliable monitoring of modal parameters during a flight vibration test using autonomous modal analysis and a kalman filter. *IFASD*, 2024.

[2] Zbigniew Zembaty, Felix Bernauer, Heiner Igel, and Karl Ulrich Schreiber. Rotation rate sensors and their applications. *Sensors (Basel, Switzerland)*, 21(16), 2021. doi: 10.3390/s21165344.

[3] Patrick Guillaume, Peter Verboven, Steve Vanlanduit, Herman Van Der Auweraer, and Bart Peeters. A poly-reference implementation of the least-squares complex frequency-domain estimator. *Proceedings of IMAC*, 21(01), 2003.

[4] Anders Brandt. *Noise and Vibration Analysis: Signal Analysis and Experimental Procedures*. John Wiley & Sons Incorporated, Newark, 2nd ed. edition, 2023. ISBN 978-1-118-96218-3.

[5] U. Fuellekrug, M. Boeswald, D. Goege, and Y. Govers. Measurement of frfs and modal identification in case of correlated multi-point excitation. *SHOCK AND VIBRATION*, 15(3-4):435–445, 2008. ISSN 1070-9622.

[6] Jurij Sodja et. al. Ground testing of the flexop demonstrator aircraft. In *AIAA Scitech 2020 Forum*, Reston, Virginia, 2020. American Institute of Aeronautics and Astronautics. ISBN 978-1-62410-595-1. doi: 10.2514/6.2020-1968.

[7] Julius Bartasevicius et. al. Flipased flight test data. 14.09.2023. URL `https://hdl.handle.net/21.15109/CONCORDA/PU4R32`.

[8] Keith Ian Soal et. al. Flutter flight testing: Using operational modal analysis to identify, track and predict flutter for safe and efficient flight test campaigns. *IFASD*, 2024.

[9] Robin Volkmar et. al. Adaptive kalman filter tracking for instantaneous aircraft flutter monitoring. *26th International Conference on Information Fusion*, June 2023.